High-throughput yeast two-hybrid library screening using next generation sequencing

Marie-Laure Erffelinck[1,2,], Bianca Ribeiro[1,2,], Maria Perassolo[1,2,3,4], Laurens Pauwels[1,2], Jacob Pollier[1,2], Veronique Storme[1,2] and Alain Goossens[1,2*]

[1]Ghent University, Department of Plant Biotechnology and Bioinformatics, Technologiepark 927, B-9052 Ghent, Belgium

[2]VIB Center for Plant Systems Biology, Technologiepark 927, B-9052 Ghent, Belgium

[3]Universidad de Buenos Aires, Facultad de Farmacia y Bioquímica, Departamento de Microbiología, Inmunología y Biotecnología, Cátedra de Biotecnología, Buenos Aires, Argentina

[4]CONICET-Universidad de Buenos Aires, Instituto de Nanobiotecnología (NANOBIOTEC), Buenos Aires, Argentina

[*]Corresponding author

E-mail: alain.goossens@psb.vib-ugent.be

[¶]These authors contributed equally to this work.

Short title: High-throughput Y2H-seq library screening

Abstract

Yeast two-hybrid (Y2H) is a well-established genetics-based system that uses yeast to selectively display binary protein-protein interactions (PPIs). To meet the current need to unravel complex PPI networks, several adaptations have been made to establish medium- to high-throughput Y2H screening platforms, with several having successfully incorporated the use of the next-generation sequencing (NGS) technology to increase the scale and sensitivity of the method. However, these have been to date mainly restricted to the use of fully annotated custom-made open reading frame (ORF) libraries and subject to complex downstream data processing. Here, a streamlined high-throughput Y2H library screening strategy, based on integration of Y2H with NGS, called Y2H-seq, was developed, which allows efficient and reliable screening of Y2H cDNA libraries. To generate proof of concept, the method was applied to screen for interaction partners of two key components of the jasmonate signaling machinery in the model plant *Arabidopsis thaliana*, resulting in the identification of several previously reported as well as hitherto unknown interactors. Our Y2H-seq method offers a user-friendly, specific and sensitive screening method that allows high-throughput identification of PPIs without prior knowledge of the organism's ORFs, thereby extending the method to organisms of which the genome has not entirely been annotated yet. The quantitative NGS readout and the incorporation of background controls allow to increase genome coverage and ultimately dispose of recurrent false positives, thereby overcoming some of the bottlenecks of current Y2H technologies, which will further strengthen the value of the Y2H technology as a discovery platform.

Introduction

Disentangling protein-protein interaction (PPI) networks is crucial for our understanding of cellular organization and function. To achieve this, a wide range of technologies to identify PPIs has been developed over the last decade [1,2]. One of the most advanced and commonly used methods to identify PPIs *in vivo* under near-physiological conditions is affinity purification coupled to mass spectrometry (AP-MS) [3-5]. Equivalent comprehensive assays to specifically identify binary PPIs include protein domain microarrays and *in vivo* protein fragment complementation assays (PCAs) [6-10]. The principle of PCA is based on the fusion of two hypothetically interacting proteins (bait and prey) to two fragments of a reporter protein. Interaction between the bait and prey proteins results in the reassembly of the reporter protein, followed by its activation. The signal readout can be bioluminescence, fluorescence or cell survival. In the popular yeast two-hybrid (Y2H) method, the bait protein is fused to the DNA binding domain (DBD) and the prey (or prey library in the case of a comprehensive Y2H screening) is fused to the activation domain (AD) of a transcription factor (TF) [11]. Upon association of the hypothetical interactors, the TF is functionally reconstituted and drives the expression of a reporter gene that can be scored by selective growth. Typically, conventional medium-throughput Y2H library screenings are subject to laborious one-by-one clonal identification of interaction partners, but today, proteome-wide mapping of PPIs demands a high-throughput approach. This led for instance to the development of a matrix-based Y2H method that bypassed the inefficient identification by DNA sequencing [12]. Collections of bait and prey strains were automatically combined and arrayed on fixed matrix positions and PPIs were scored as visual readouts. A major drawback of this strategy is the need for pre-assembled libraries based on defined gene models and expensive robotics that are not accessible to every researcher.

Clonal identification of Y2H screening with DNA sequencing has a tremendous negative effect on the efficiency, cost and labor of the method. Furthermore, given the labor-penalty involved with increasing transformation titers, the clonal identification of Y2H interactions is usually not compatible with quantitative assessment of PPI abundances. Therefore, replacing the conventional Y2H screening strategy with a pool-based selection and global identification by NGS, can have three major implications: (i) cost reduction by high-capacity sequencing, (ii) higher sensitivity and (iii) quantification of the abundance of bait-specific interactions. The lab of Marc Vidal pioneered the implementation of the NGS technology for massive parallel Y2H screening in the Stitch-Seq method, mainly to map the human interactome. Herein, single amplicons, concatenating sequences of potentially interacting proteins, serve as template for NGS [13]. Nonetheless, this method remains laborious because it requires clonal isolation and several PCR rounds for PPI identification for each selected colony. The lab of Ulrich Stelzl developed the Y2H-seq method, thereby illustrating the advantage of NGS for Y2H towards scalability by mapping the protein methylation interactome [14]. In this strategy, the use of barcode indexing enables simultaneous sequencing of interacting preys of multiple separate baits in a single Illumina run. This strategy is based on mixing bait and prey pools prior mating, followed by selective growth, and deep-sequencing, but still requires a post-screen binary testing of interacting baits with each of the identified preys. The use of barcodes was further exploited in the Barcode Fusion Genetics-Yeast Two-Hybrid (BFG-Y2H) method. This matrix-Y2H strategy uses Cre-recombinase to create intracellular chimeric barcodes that are derived from protein pairs, thereby enabling immediate identification and quantification of each interaction pair through NGS [15]. Prior to screening and NGS, isolation and sequencing of each barcoded bait and prey clone are essential to associate barcodes to ORFs, which may pose a cost

92 restriction for massive screening purposes. The latter was addressed in CrY2H-seq, which
93 introduced a Cre-recombinase interaction reporter that endorses fusion of the coding
94 sequences of two interacting proteins, followed by NGS to identify these interactions *en*
95 *masse* [16]. The latter method was employed to uncover the transcription factor
96 interactome of *A. thaliana*.
97 All of the above-mentioned Y2H-NGS strategies focus on increased capacity, efficiency
98 and sensitivity, although they may face some lack in specificity or do not fully exploit the
99 quantification potential of NGS coupled to Y2H. Furthermore, construction of full-length ORF
100 libraries are necessary, thereby restricting these methods to organisms of which the
101 genomes are well annotated or to 'defined' gene models, which for instance cannot take
102 alternative splicing, alternative start codon use or transcript processing into account.
103 Here, we discuss a user-friendly and standardized Y2H-NGS workflow ('Y2H-seq'),
104 complementary to the matrix-Y2H approaches, which allows rapid identification of
105 interaction partners of a bait of interest in the organism of choice without the need for
106 expensive robotics. The Y2H-seq screening method generates a quantitative readout that,
107 through the use of control screens, allows to eliminate false-positive PPIs to boost the
108 specificity of the method and thereby avoiding unnecessary downstream experimental
109 binary interaction verification. Furthermore, the method is not dependent on predefined
110 and prefabricated ORF libraries but on cDNA libraries, and is therefore principally applicable
111 to every organism regardless of the annotation status of its genome. The functionality of our
112 methodology is validated here by implementing it on two well-studied members of the
113 jasmonate (JA) signaling cascade in the model plant *Arabidopsis thaliana*, i.e. TOPLESS (TPL)
114 and Novel Interactor of JAZ (NINJA), respectively encoded by the loci AT1G15750 and
115 AT4G28910 [17-25].

Material and methods

Gene Cloning

All cloning was carried out by Gateway® recombination (Thermo Fisher Scientific, Waltham, MA, USA). The full-length coding sequence of *IAA17* was PCR-amplified (for primers, see S2 Table) and recombined in the donor vector pDONR221. All other entry clones had previously been generated [17,26].

Binary Y2H analysis

Y2H analysis was performed as described [27] using the GAL4 system [27], in which bait and prey were fused to the GAL4-AD or GAL4-BD via cloning into pDEST^{TM}22 or pDEST^{TM}32, respectively. The *Saccharomyces cerevisiae* PJ69-4α yeast strain [28] was co-transformed with bait and prey constructs using the polyethylene glycol (PEG)/lithium acetate method. Transformants were selected on SD medium lacking Leu and Trp (Clontech, France). Three individual colonies were grown overnight in liquid cultures at 30°C and 10- or 100-fold dilutions were dropped on control (SD-Leu-Trp) and selective media (SD-Leu-Trp-His).

Y2H screening

Yeast transformation was performed as described by Cuéllar-Pérez *et al.*, (2013) [27]. The *S. cerevisiae* PJ69-4α yeast strain was transformed in two transformation rounds, respectively with 0.5 µg of bait plasmid DNA and 50 µg of cDNA prey library plasmid DNA using the PEG/lithium acetate method. At least 10^6 transformants were plated on control (SD-Leu-Trp) and selective media lacking Leu, Trp and His supplemented with 5 mM 3-AT (Sigma-Aldrich, Saint Louis, MO, USA).

Y2H cDNA library used to perform the Y2H screening

The ProQuest two-hybrid cDNA library was generated by cDNA synthesis from RNA extracted from *A. thaliana* suspension cells AT7, cloned into pEXP-AD502 vector (ProQuest), equivalent to pDEST^{TM}22 vector (Thermo Fisher Scientific) and electroporated in the DH10B-Ton A (T1 and T5 phage resistance) cells (Thermo Fisher Scientific). The average insert size was 1.1 kb and the number of primary clones was 5.3 x 10^6 cfu with a 100% insert coverage.

Sanger sequencing

A minimum of ten random colonies of the Y2H screening plates were streaked out on solid SD-Leu-Trp-His selective medium with 5mM 3-AT (Sigma-Aldrich, Saint Louis, MO, USA) and incubated for 48 h at 30°C. Each streaked out colony was inoculated in liquid SD-Leu-Trp-His selective medium and incubated overnight at 30°C at 230 rpm. Subsequent yeast plasmid isolation was carried out using the Zymoprep^{TM} Yeast Plasmid Miniprep I Kit (Zymo Research, Irvine, CA, USA) according to the manufacturer's instructions. The cDNA inserts of the prey plasmids (pDEST^{TM}22-insert) were PCR-amplified using backbone-specific primers (S2 Table) and Sanger-sequenced.

Semi-quantitative qPCR

Colonies of the Y2H screening plates were dissolved and pooled in 10-15 mL of ultrapure water and plasmids were collected using the Zymoprep^{TM} Yeast Plasmid Miniprep II kit (Zymo Research, Irvine, CA, USA). Prey constructs were amplified via PCR using Q5® High-Fidelity DNA Polymerase (New England Biolabs, Ipswich, MA, USA) and generic pDEST^{TM}22 primers that bind to the GAL4AD and the region flanking the attR1 site (S2 Table). The following program was used: initial denaturation (98°C, 30 s), 35 amplification cycles (denaturation 98°C, 10 s; annealing 55°C, 30 s; elongation 72°C, 2.5 min), final extension

(72°C, 5 min). The PCR mixture was purified using the CleanPCR kit (CleanNA, Alphen aan den Rijn, The Netherlands) and 40 ng of the purified PCR product was used for semi-quantitative qPCRs, which were carried out with a Lightcycler 480 (Roche Diagnostics, Brussels, Belgium) and the Lightcycler 480 SYBR Green I Master kit (Roche). Specific primers (S2 Table) and GoTaq® DNA polymerase (Promega, Fitchburg, WI, USA) were used for amplification of 40 ng of purified PCR product with the following program: initial denaturation (95°C, 5 min), 40 amplification cycles (denaturation 95°C, 30 s; annealing 60°C, 30 s; elongation 72°C, 60 s), final extension (72°C, 5 min). As a reference, a short sequence originating from the AD of pDEST^{TM}22 was used. For the relative quantification with the reference gene, qBase was used [29].

NGS data processing

The samples were sequenced by Illumina HiSeq 2000 125-bp paired-end reads. Data mapping and filtering were carried out through an in-house generated pipeline. To avoid sequencing artifacts such as read errors, primers, adapter and vector sequence contamination and PCR bias, a quality check was performed on the raw sequencing data. The quality control and trimming were performed with Trimmomatic [30]. Subsequently, the processed sequencing reads were mapped against the *Arabidopsis* reference genome, downloaded from TAIR (The Arabidopsis Information Resource, http://arabidopsis.org), by TopHat [31], which uses the Bowtie program as an alignment engine. In addition, TopHat requires SAM (Sequence Alignment/Map) tools to be installed. The cufflinks program was used to count the expression of each gene and report it as raw reads and FPKM. To determine possible interactors, following steps were taken. Genes with less than six read counts were not considered. Zero counts in the negative control sample were replaced by 1

to avoid division by 0. These genes were flagged to keep track of these imputations. FPKM values were calculated for each gene in both the sample and the negative control. Subsequently, the SNR was calculated for each gene as the ratio of the sample FPKM value to the negative control FPKM value. Genes with an $SNR_{NINJA/EMPTY}$ or $SNR_{TPL\text{-}N/EMPTY}$ higher than the arbitrary threshold of 11, were considered to be potential interaction partners of the bait gene.

Results

Selection of baits

JAs are phytohormones that regulate the plant's defense and modulate several developmental processes. The production of JAs via the oxylipin biosynthetic pathway leads to the accumulation of bioactive (+)-7-*iso*-jasmonoyl-L-isoleucine (JA-Ile). JA-Ile functions as a ligand between the F-box protein coronatine insensitive 1 (COI1) and the JA-ZIM (JAZ) repressor proteins, thereby promoting ubiquitination and subsequent proteasomal degradation of the JAZ proteins [32,33]. Together with the TIFY8, peapod (PPD) and ZIM proteins, the JAZ proteins belong to the TIFY super-family [32,34-37]. A key regulator in JA signaling in *A. thaliana* is the basic helix-loop-helix (bHLH) TF MYC2, encoded by the locus AT1G32640 [38,39]. In the absence of JA-Ile, MYC2 can physically interact with the JAZ proteins via the Jas motif, which in turn recruit the transcriptional repressor TPL and TPL-related proteins (TRPs) through the adaptor protein NINJA [17]. NINJA acts as a transcriptional repressor that harbors an intrinsic TPL-binding ETHYLENE RESPONSE FACTOR (ERF)-associated amphiphilic repression (EAR) motif mediating its activity (Fig 1) [17]. NINJA can also interact with non-JAZ TIFY proteins, demonstrating its role in processes other than JA signaling [17,34,37,40,41]. Likewise, TPL is associated with various cellular processes

208 through its capacity to interact with a compendium of diverse proteins [17-24,37]. For
209 instance, TPL can bind to PEAPOD proteins through the adapter proteins KIX8 and KIX9 to
210 negatively regulate meristemoidal division in *A. thaliana* [37]. A role for TPL modulating
211 brassinazole resistant 1 (BZR1)-regulated cell elongation and brassinosteroid-mediated
212 control of shoot boundaries and root meristem development through interaction with the TF
213 bri1-ems-suppressor 1 (BES1) has been described [22,24]. TPL can also be recruited by CC-
214 type glutaredoxins to target TGA-dependent promoters to control development- and stress-
215 associated processes.

216 Because various direct interactors have been described for both NINJA and TPL proteins
217 and because these are currently still heavily investigated for potential novel roles and links
218 with different signaling pathways and cellular processes, NINJA and TPL were chosen as ideal
219 bait proteins to develop, establish and validate our Y2H-seq methodology. Notably, whereas
220 we used the full-length ORF of NINJA as a bait, for TPL only the amino-terminal region (AA 1-
221 188; TPL-N) was used as a bait because this domain contains the lissencephaly homologous
222 (LisH) dimerization and C-terminal to LisH (CTLH) motifs, which are together required and
223 sufficient for interaction with transcriptional repressors through their EAR motif.

224

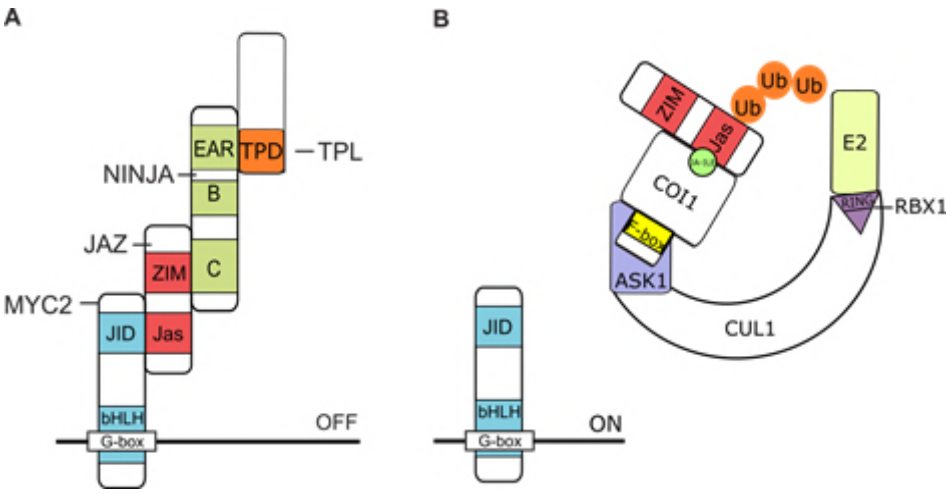

225

Figure 1. Function of TOPLESS and NINJA in JA signaling in *A. thaliana*. (A) In the absence of JAs, bHLH-type MYC TFs interact with the Jas domain of JAZ proteins that in turn interact with NINJA via their ZIM domain. The EAR motif of NINJA is essential for recruitment of the TPL co-repressors through the TPL domain (TPD). (B) In the presence of JA-Ile, JAZ proteins interact with the ubiquitin E3 ligase SCF^{COI1} complex, leading to the proteasomal degradation of JAZs and consequent release of the NINJA–TPL complex from the MYC TFs, which leads to the transcriptional activation of JA-responsive genes by de-repressed MYC TFs.

The Y2H-seq flow-chart

An illustration of the general workflow of our Y2H-Seq strategy is given in Figure 2. As indicated above NINJA and TPL-N were used as baits and a Y2H cDNA library originating from *A. thaliana* AT7 suspension cells was used as prey.

After transformation of the Y2H reporter strain PJ69-4α with the bait plasmids, a first checkpoint is introduced, in which the bait strains were individually co-transformed with positive and negative control prey expression clones to verify functional expression of the baits, to exclude possible auto-activation and to corroborate binding with previously reported interaction partners (Fig 1). Next, the bait strains were used for Y2H-seq screening with the *A. thaliana* Y2H cDNA prey library. Simultaneously, a control screening was performed with the empty expression vector, which will hereafter be referred to as EMPTY. Subsequent to five days of selective growth of the transformed yeast cells, the prey cDNA inserts of about ten individual yeast colonies per screen were Sanger-sequenced (Fig 1). This second checkpoint allowed us to confirm the retrieval of reported interactors as preys. Subsequently, all yeast colonies that survived selective growth were pooled per screen and the cDNA inserts of the prey plasmid pools were amplified by PCR. A third checkpoint consisted of a qPCR analysis with specific primers for genes corresponding to known bait interactors, which allows to assess the representation of known interactors in both screens

252 in a quantitative manner (Fig 1). Prey abundance was quantified relative to that in the *A.*
253 *thaliana* Y2H cDNA library.

254 Upon complying the expectations of all three checkpoints, the amplicons of the pooled
255 prey cDNA inserts were sequenced by NGS (Illumina HiSeq 2000 sequencing, 125-bp paired-
256 end reads). The NGS-output was analyzed by an adapted RNA-Seq data processing pipeline,
257 providing a quantitative selection of known and potentially new interactors of NINJA and
258 TPL-N, using the EMPTY screen as control to eliminate false-positive interactions and to
259 correct for the abundance of each prey represented by the Y2H cDNA library.
260

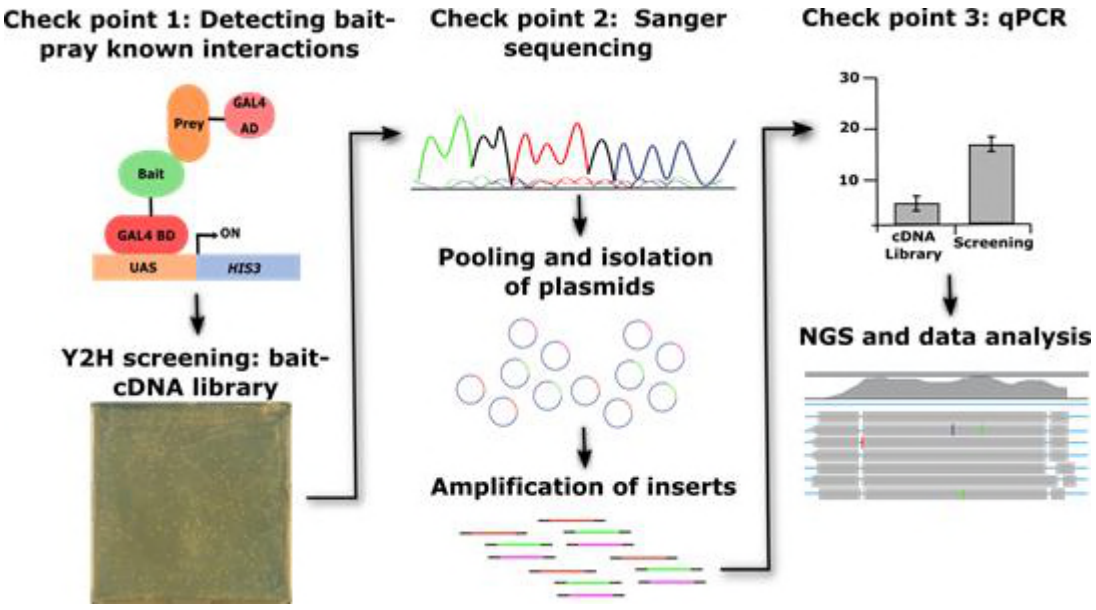

261

262 **Figure 2. Y2H-seq workflow.**

263

264 **Y2H-seq checkpoints**

265 ***Checkpoint 1: exploring auto-activation and functionality of the bait strains***

266 The bait strains were individually co-transformed with positive and negative control preys
267 (Fig 3 and S1 Table) to determine the level of auto-activation of the bait strain and to check

268 whether the bait protein is functionally expressed and consequently can bind previously

269 reported interaction partners [17,25,37].

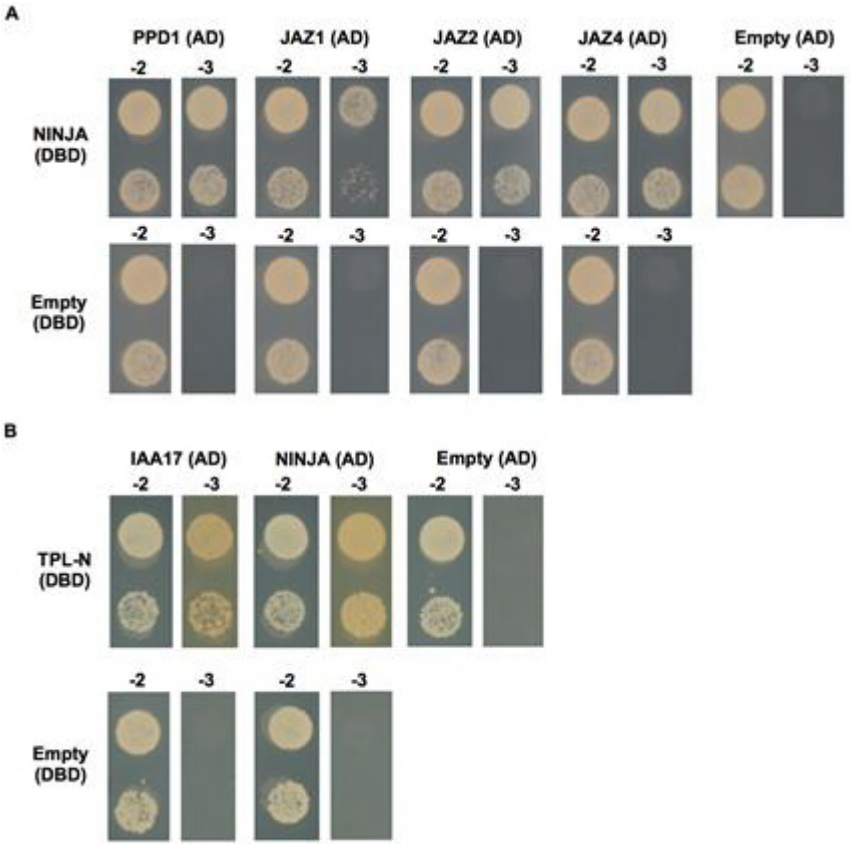

270

271 **Figure 3. Y2H of the NINJA and TPL-N bait proteins with positive and negative control prey**
272 **proteins.** Y2H analysis of NINJA and TPL-N baits, fused to the DBD, and preys, fused to the AD, grown
273 for 2 days on selective medium Synthetic Defined (SD)-Leu-Trp-His (-3). Transformed PJ69-4α yeast
274 strains were also grown for 2 days on SD-Leu-Trp (-2) medium to confirm growth capacity. Direct
275 interaction was confirmed between **(A)** NINJA and PPD1, JAZ1, JAZ2 and JAZ4, and **(B)** TPL-N and
276 auxin/indole-3-acetic acid 17 (IAA17) and NINJA.
277
278 As expected, the binary interaction between the NINJA bait and the preys PPD1, JAZ1, JAZ2
279 and JAZ4 was confirmed (Fig 3A). Likewise, the TPL-N bait strain showed interaction with the
280 preys auxin/indole-3-acetic acid 17 (IAA17) and NINJA (Fig 3B). Furthermore, neither of the
281 bait strains exhibited auto-activation, which indicated that NINJA as well as TPL-N were
282 functionally expressed in the bait strains.

283 ***Checkpoint 2: Evaluation of quality of Y2H-seq screening with bait strains by Sanger***

284 ***sequencing***

285 For the actual Y2H screening, the bait strains were supertransformed with the *A. thaliana*

286 Y2H cDNA prey library, followed by transformation efficiency assessment and five days of

287 selective growth (Fig 4 and S1 Table). A minimum transformation efficiency of 1 x 10^6

288 screened yeast colonies should be attained for a full Y2H cDNA library screening coverage.

289 This benchmark was achieved for all Y2H screenings we performed (Table 1).

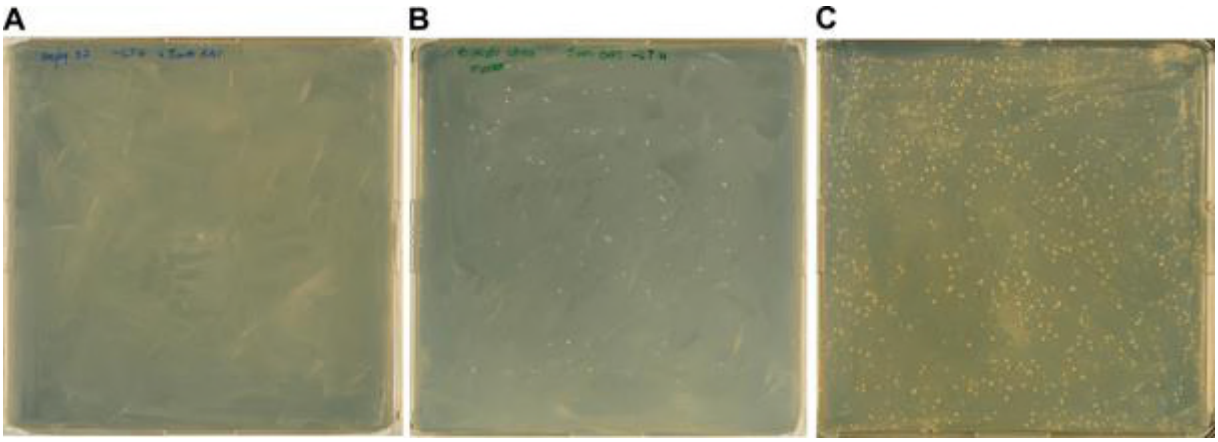

290

291 **Figure 4. Y2H-seq selective growth.** (A-C) The EMPTY (A), NINJA (B), and TPL-N (C) Y2H-seq
292 screenings were performed on selective SD-Leu-Trp-His + 5mM 3-AT.
293

294 **Table 1. Transformation efficiency of Y2H screenings using EMPTY, TPL-N and NINJA as baits.** To
295 ensure a full screening coverage of the *A. thaliana* Y2H cDNA library, screening of at least 1 x 10^6
296 yeast colonies is advised [42].

Bait	Transformation efficiency (# of colonies screened)
EMPTY	1.23 x 10^7
NINJA	3.85 x 10^6
TPL-N	2.05 x 10^7

297

298 A minimum of ten individual colonies per screening were isolated, plasmids purified and the

299 cDNA inserts of the prey plasmids Sanger-sequenced. In this second checkpoint, several

300 known interactors could already be identified (Table 2). The ten sequences originating from

301 the NINJA screening corresponded to two unique interaction partners that were previously

described as NINJA interactors [17]. Likewise, the 12 prey sequences that corresponded to potential interactors of TPL-N were derived from six different, all known interactors [18].

Table 2. Sanger sequencing of isolated NINJA and TPL-N preys.

# Colonies	Gene description	Gene ID
NINJA		
8	*A. thaliana* jasmonate-ZIM-domain protein 1 (JAZ1)	AT1G19180
1	*A. thaliana* protein PEAPOD2 (PPD2)	ATt4G14720
TPL-N		
4	*A. thaliana* indole-3-acetic acid inducible 2 (IAA2)	AT3G23030
3	*A. thaliana* indole-3-acetic acid inducible 28 (IAA28)	AT5G25890
2	*A. thaliana* AGAMOUS-like 18 (AGL18)	AT3G57390
1	*A. thaliana* indole-3-acetic acid inducible 4 (IAA4)	AT5G43700
1	*A. thaliana* indole-3-acetic acid inducible 30 (IAA30)	AT3G62100
1	*A. thaliana* indole-3-acetic acid inducible 9 (IAA9)	AT5G65670

Checkpoint 3: semi-quantitative qPCR, a complementary approach to evaluate the quality of a Y2H-seq screening

In a third checkpoint, the quality of the Y2H-seq screening was further assessed. All selectively grown yeast colonies were pooled per screening (Fig 2) and cDNA inserts of the prey plasmid pools were PCR-amplified with vector-specific primers (S2 Table). To examine whether potential interaction partners of the baits were overrepresented relative to the cDNA library control, a qPCR was performed using prey-specific qPCR primers (S2 Table). In the NINJA screen, compared to the control library, the genes encoding JAZ1, JAZ2, JAZ12, TIFY8 and PPD1 were overrepresented (Fig 5), in agreement with previous literature reports [17,34]. Hence, this shows the value of this qPCR assay set-up as a final checkpoint before the actual Y2H-seq analysis, at least for baits with a limited set of known interactors.

In contrast to NINJA, TPL can interact with potentially hundreds of proteins [18]. Of the EAR-motif containing proteins known to interact with TPL and identified in the second

checkpoint, only enrichment of IAA30 in the TPL-N pool could be observed (Fig 6, Table 2). Y2H cDNA library screenings are prone to false negatives, i.e. missing interactions, due among others to aberrant folding, clones with truncated genes or absence of the gene in the cDNA library. In the case of TPL-N, for example, the *NINJA* clone that is represented by the *A. thaliana* Y2H cDNA library was found to be truncated and missing the EAR domain necessary for binding with TPL-N. Therefore, critical analysis of theY2H cDNA library content prior and post Y2H screening remains crucial to critically interpret the outcome of a Y2H screen.

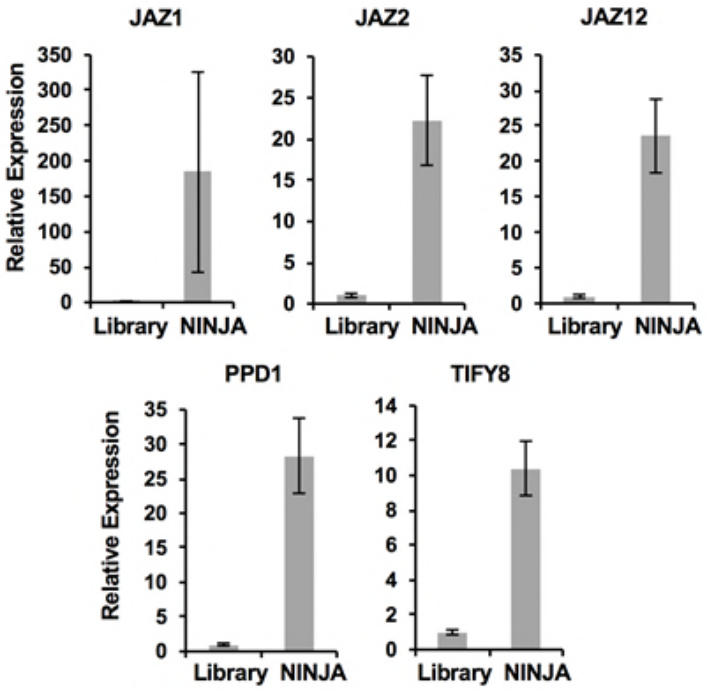

Figure 5. qPCR assessment of the NINJA Y2H-seq screen. *JAZ1*, *JAZ2*, *JAZ12*, *TIFY8* and *PPD1* were overrepresented in the PCR products of the NINJA screening compared to the PCR products of the *A. thaliana* cDNA library (Library).

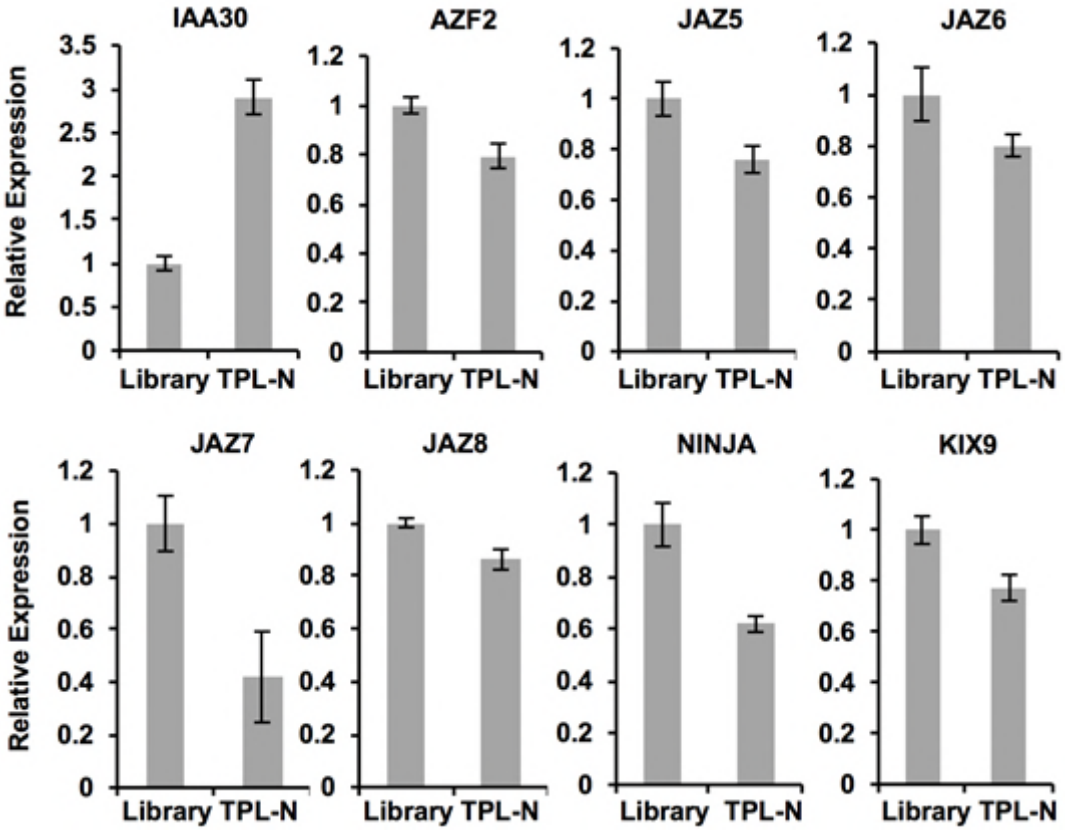

Figure 6. qPCR assessment of the TPL-N Y2H-seq screening. Only *IAA30* was overrepresented in the PCR products of the TPL-N screening compared to the *A. thaliana* cDNA library (Library) cDNA insert amplicons.

Beyond the checkpoints: NGS of the amplified prey cDNA inserts

The prey pool amplicons of the EMPTY, NINJA, and TPL-N screenings were used as input for NGS by Illumina HiSeq 2000 (125-bp paired-end reads). Here, we used a pipeline relying on TopHat for read mapping and Cufflinks for gene expression quantification. The method presented here aims to compare the gene expression levels of the NINJA and TPL-N Y2H-seq screens with the EMPTY control screen to enrich for specific interaction partners while maximally avoiding the retrieval of false-positive interactions.

First, a quality check was performed on the raw reads. Thereby, adapters, low-quality sequences and partial vector sequences were trimmed. Concomitantly, paired-end and orphan single-end reads were split. The processed reads were then mapped to the reference

348 genome (TAIR10) using TopHat. To avoid overestimation of short genes, only one mate-pair
349 per read was used for mapping. The resulting alignments were used as input for Cufflinks,
350 which generates the raw expression quantification data for each of the analyzed raw
351 sequencing files. For the subsequent analysis of the raw expression data, a Y2H-seq pipeline
352 was drafted in R-studio.

353 Mapped genes in the TPL-N and NINJA Y2H screenings with raw read counts less than six
354 were eliminated. Genes in the EMPTY screening that had no raw read counts were given an
355 arbitrary value of 1 and flagged as imputed. After calculating the Fragments Per Kilobase of
356 Exon Per Million Fragments Mapped (FPKM) values, the signal to noise ratio (SNR) was
357 defined for NINJA and TPL-N compared to EMPTY. Intuitively, one would expect little NGS
358 data to be derived from the EMPTY screening, given that no yeast cells survived selective
359 growth (Fig 4). However, this was not the case and can be explained by the pooling method
360 employed here: 'scraping' all yeast cells from the selection plates includes also dead or
361 nearly dead cells that may still contain intact prey plasmids. Hence, genes with a high
362 representation in the cDNA library, and thus genes with a high expression level in
363 *Arabidopsis* suspension cells, are identified in the EMPTY NGS data set.

364 Next, to allow setting relevant arbitrary thresholds, the 99.5th percentiles of $SNR_{NINJA/EMPTY}$
365 and $SNR_{TPL\text{-}N/EMPTY}$ were calculated, leading to thresholds of 7.2 for NINJA and 6.0 for TPL-N
366 screenings, respectively (Tables 3 and 4). With this first threshold, overall, from the 71
367 potential interactors of NINJA, seven were known to be interactors [17,34], whereas for TPL-
368 N, 12 out of the 51 potential interactors had been previously reported [25].

369 When super-implying a second threshold, in this case of >100 on the $FPKM_{NINJA}$ and
370 $FPKM_{TPL\text{-}N}$ values, nearly all retained interactors were either reported already or very
371 plausible. Indeed, in the case of NINJA, only TIFY-domain containing proteins were retained

(Fig 6, Table 3). In the case of TPL-N, all but one of the retained proteins using this second threshold contained an EAR-motif [43], the conventional TPL recruitment domain (Fig 7, Table 4), and also includes proteins not yet individually reported as TPL-interactors, but belonging to multigene families such as the AGAMOUS-LIKE (AGL) and INDOLE-3-ACETIC ACID INDUCIBLE (IAA) proteins, many members of which have already been reported as TPL interactors [18,25]. Together, this demonstrates the robustness and potential of the designed Y2H-seq platform.

Table 3. Signal-to-noise ratio of the FPKM values of NINJA and EMPTY Y2H-seq screenings. Genes with $SNR_{NINJA/EMPTY}$>7.2 were retained, listed and ranked from high to low SNR. Flagged genes are italicized. Previously reported interactors of NINJA are indicated in bold. Potential interactors that were tested for binary interaction in further validation assays are underlined.

	Gene ID	Gene-length	$FPKM_{EMPTY}$	$FPKM_{NINJA}$	SNR_{FPKM}	Gene Alias	Full-length	TIFY domain
	$FPKM_{NINJA}$>100							
1	**AT3G17860**	1588	0,731	1212,639	1659,075	JAI3/JAZ3/TIFY6B	Y	Y
2	**AT1G19180**	1329	27,074	20257,141	748,213	AtJAZ1/TIFY10A	Y	Y
3	**AT1G74950**	1280	4,081	2569,920	629,798	JAZ2/TIFY10B		Y
4	**AT5G13220**	1375	5,065	2735,323	540,063	JAS1/JAZ10/TIFY9	Y	Y
5	**AT4G14713**	1503	1,544	375,437	243,081	PPD1/TIFY4A	Y	Y
6	**AT1G17380**	1133	1,537	124,895	81,277	JAZ5/TIFY11A	Y	Y
7	**AT4G14720**	1568	3,701	294,079	79,455	PPD2/TIFY4B	Y	Y
	$FPKM_{NINJA}$<100							
8	*AT4G36480*	2058	0,282	28,960	102,697	ATLCB1/EMB2779		
9	AT1G34340	1833	0,950	47,346	49,847			
10	AT3G06850	1730	1,342	33,645	25,074	BCE2/DIN3/LTA1		
11	AT4G05553	336	1,727	36,306	21,020		Y	
12	AT5G47810	1684	4,480	64,989	14,506	PFK2	Y	
13	AT3G03680	3308	0,175	2,213	12,612			
14	AT3G15760	843	0,688	8,269	12,011		Y	
16	AT3G02830	1695	0,342	4,113	12,011	PNT1/ZFN1	Y	
17	*AT2G34160*	636	0,912	10,412	11,411		Y	
18	AT4G17080	2053	0,283	3,056	10,810			
19	*AT3G06550*	2145	0,271	2,762	10,210	RWA2		
20	AT1G58150	276	2,103	20,205	9,609		Y	
21	AT1G29890	1901	0,916	8,801	9,609	RWA4		
22	AT2G33820	936	0,620	5,958	9,609	ATMBAC1	Y	
23	*AT1G73340*	1711	0,339	3,259	9,609		Y	
24	AT5G67440	2662	0,218	2,095	9,609	MEL2/NPY3		
25	AT1G32440	1908	0,304	2,740	9,009	PKp3		

26	*AT3G49350*	2220	0,261	2,355	9,009		
27	AT2G44830	2399	0,242	2,179	9,009		
28	AT5G27390	1040	1,116	9,719	8,708		Y
29	AT2G30105	1377	0,421	3,544	8,408		
30	AT3G61790	1407	0,412	3,468	8,408		
31	AT4G39140	1600	0,363	3,050	8,408		
32	AT4G37880	1608	0,361	3,035	8,408		
33	AT1G26260	1622	0,358	3,008	8,408	CIB5	
34	AT4G02100	2085	0,278	2,340	8,408		
35	AT5G16000	2323	0,250	2,101	8,408	AtNIK1	
36	*AT2G23450*	2387	0,243	2,044	8,408		
37	AT3G42660	2862	0,203	1,705	8,408		
38	*AT1G13370*	648	0,896	6,992	7,807		Y
39	AT1G66670	1196	0,485	3,788	7,807	CLPP3/NCLPP3	Y
40	AT2G32340	1256	0,462	3,607	7,807		Y
41	AT1G10660	1648	0,352	2,749	7,807		
42	AT3G16090	2120	0,274	2,137	7,807	AtHrd1A	
43	AT4G12120	2404	0,241	1,885	7,807	ATSEC1B	
44	AT3G23660	2568	0,226	1,764	7,807		
45	AT1G31440	1870	0,621	4,660	7,507		
46	AT3G44716	592	0,980	7,065	7,207		Y
47	AT3G60640	643	0,903	6,505	7,207	ATG8G	Y
48	AT2G34980	912	0,636	4,586	7,207	SETH1	Y
49	*AT5G28330*	974	0,596	4,294	7,207		Y
50	*AT4G25600*	1165	0,498	3,590	7,207		
51	AT2G18162	1231	0,471	3,398	7,207	CPuORF1	Y
52	AT3G04730	1279	0,454	3,270	7,207	IAA16	Y
53	AT4G26070	1342	0,432	3,117	7,207	ATMEK1/MKK1N	Y
54	AT1G03687	1428	0,406	2,929	7,207		
55	AT1G06910	1528	0,380	2,737	7,207	TRFL7	
56	*AT1G52630*	1537	0,378	2,721	7,207		Y
57	AT1G18570	1654	0,351	2,529	7,207	AtMYB51/BW51A	
58	*AT2G33580*	2239	0,259	1,868	7,207	LYK5	
59	AT5G04550	2580	0,225	1,621	7,207		
60	*AT4G03560*	2674	0,217	1,564	7,207	ATCCH1/ATTPC1	
70	AT4G02020	2876	0,202	1,454	7,207	EZA1/SDG10	
71	AT3G13690	3321	0,175	1,259	7,207		

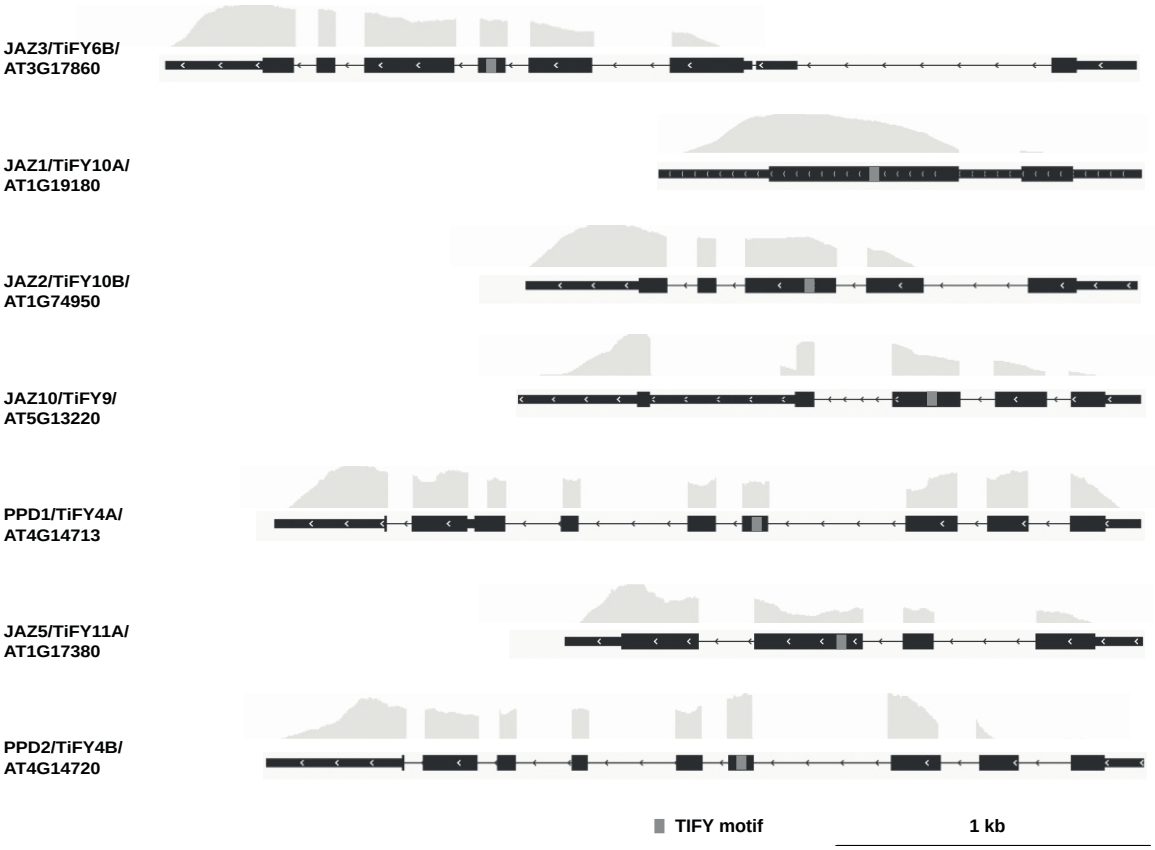

Figure 6. Deepseq coverage of the NINJA interactors using cutoff of $SNR_{NINJA/EMPTY}$>7.2 and $FPKM_{NINJA}$>100. The depth of the deepseq coverage for each gene, visualized by the coverage track, is aligned to the gene model. Coding sequences are represented by thick black boxes, 5' and 3' untranslated regions by thin black boxes and introns by thin black lines, respectively. The light grey boxes in the gene model correspond to the TIFY motif.

Table 4. Signal–to-noise ratio of the FPKM values of TPL-N and EMPTY Y2H-seq screenings. Genes with $SNR_{TPL-N/EMPTY}$>6 were retained, listed and ranked from high to low SNR. Flagged genes are italicized. Previously reported interactors of TPL are indicated in bold. Potential interactors that were tested for binary interaction in further validation assays are underlined. A 'Y' in bold font indicates the presence of an EAR domain in the wrong frame or in an untranslated region of the gene.

	Gene ID	Gene-length	$FPKM_{EMPTY}$	$FPKM_{N-TPL}$	SNR_{FPKM}	Gene Alias	Full-length	EAR domain
	$FPKM_{N-TPL}$>100							
1	**AT5G25890**	873	11,301	3997,602	353,736	IAA28/IAR2	Y	Y
2	**AT3G23030**	941	49,339	8581,581	173,933	IAA2	Y	Y
3	**AT5G43700**	1168	0,994	111,604	112,307	ATAUX2-11/IAA4	Y	Y
4	**AT4G28640**	1202	20,761	1121,873	54,037	IAA11	Y	Y
5	**AT4G29080**	1337	4,341	219,498	50,568	IAA27/PAP2	Y	Y
6	**AT3G15540**	970	7,180	266,613	37,135	IAA19/MSG2	Y	Y
7	**AT1G04250**	1087	249,863	8692,277	34,788	AXR3/IAA17	Y	Y
8	AT3G50000	1467	19,384	543,833	28,055	ATCKA2	Y	

9	**AT2G33310**	1820	64,093	1054,613	16,454	IAA13	Y	Y
10	AT2G46990	655	9,746	158,039	16,215	IAA20	Y	Y
11	**AT5G13790**	962	15,685	198,181	12,635	AGL15	Y	Y
	$FPKM_{N\text{-}TPL}$<100							
12	AT3G54390	1341	3,0294	69,6555	22,9933		Y	
13	***AT4G37940***	715	0,8117	15,1114	18,6177	AGL21	Y	
14	*AT2G40260*	1233	0,4707	8,1976	17,4165		Y	
16	*AT3G58820*	1391	0,4172	5,2619	12,6120			**Y**
17	**AT1G51950**	1539	4,9022	56,1646	11,4570	IAA18	Y	Y
18	**AT1G04100**	1254	1,3884	15,8426	11,4108	IAA10	Y	Y
19	AT3G05670	3090	0,9391	9,2492	9,8493			Y
20	AT4G31620	1809	0,9624	9,2481	9,6091			**Y**
21	AT2G33550	1194	8,2629	77,0636	9,3265			Y
22	AT1G08290	1760	0,3297	2,9705	9,0085	WIP3		
23	AT3G19860	1288	3,1540	25,7074	8,1506	bHLH121	Y	
24	AT5G25160	959	1,2103	9,4494	7,8074	ZFP3	Y	Y
25	AT5G47110	1088	1,0668	8,3290	7,8074	LIL3:2		
26	AT3G04730	1279	0,4537	3,5426	7,8074	IAA16		Y
27	AT5G04550	2580	0,2249	1,7562	7,8074			
28	AT3G15760	843	0,6884	4,9614	7,2068		Y	
29	AT1G12270	1949	0,5955	4,2919	7,2068	Hop1		
30	AT3G47980	1097	0,5290	3,8126	7,2068			**Y**
31	AT1G02650	1542	0,3764	2,7124	7,2068			
32	AT2G38950	2482	0,2338	1,6851	7,2068			
33	AT3G19070	1041	1,6725	11,7184	7,0066			**Y**
34	AT1G28300	1317	0,8813	6,0868	6,9066	AtLEC2		**Y**
35	AT3G56250	669	0,8675	5,7308	6,6063		Y	
36	*AT1G01030*	1905	0,3046	2,0126	6,6063	NGA3		**Y**
37	AT1G61900	1913	0,3034	2,0041	6,6063			**Y**
38	AT1G79950	3123	0,1858	1,2276	6,6063			
39	AT3G43575	4332	0,1340	0,8850	6,6063			
40	AT5G36870	5616	0,2067	1,3033	6,3060	ATGSL09/atgsl9		
41	AT2G30540	680	4,2672	26,6529	6,2459			
42	AT2G38110	1845	4,0891	25,5028	6,2367	ATGPAT6		**Y**
43	AT2G25180	1980	3,2241	19,8913	6,1695	ARR12/AtARR12		**Y**
44	*AT1G53030*	530	1,0950	6,5762	6,0057			
45	*AT1G13680*	1180	0,4918	2,9537	6,0057			
46	*AT4G19540*	1215	0,4776	2,8686	6,0057	INDH/INDL	Y	
47	AT3G56160	1600	0,3627	2,1784	6,0057			
48	*AT5G03570*	1673	0,3469	2,0833	6,0057	ATIREG2/FPN2		
49	AT3G59150	1866	0,3110	1,8678	6,0057		Y	
50	*AT4G03560*	2674	0,2170	1,3034	6,0057	ATCCH1/ATTPC1/FOU2		
51	AT3G03680	3308	0,1754	1,0536	6,0057			

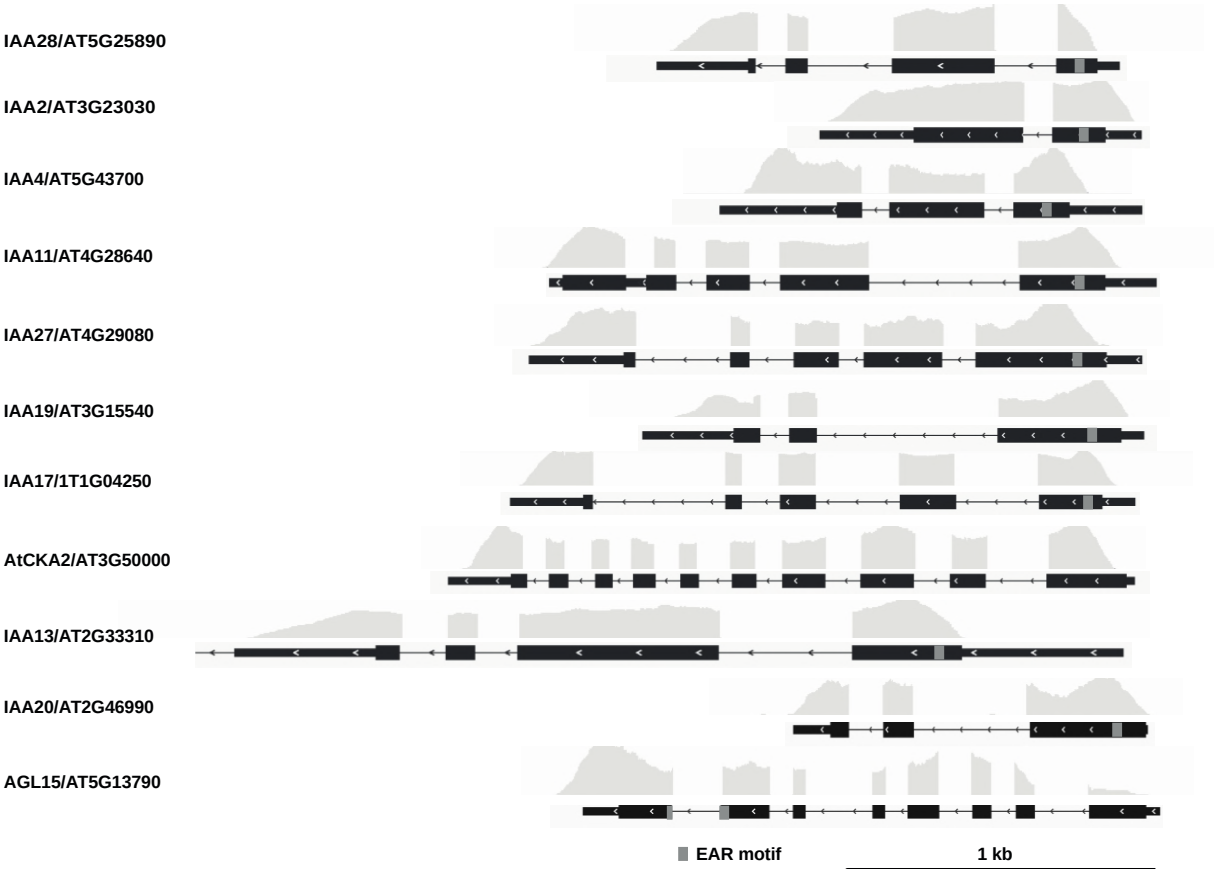

Figure 7 Deepseq coverage of the N-TPL interactors using cutoff of $SNR_{N\text{-}TPL/EMPTY}$>6 and **$FPKM_{N\text{-}TPL}$>100.** The depth of the deepseq coverage for each gene, visualized by the coverage track, is aligned to the gene model. Coding sequences are represented by thick black boxes, 5' and 3' untranslated regions by thin black boxes and introns by thin black lines, respectively. The grey boxes in the gene model correspond to the EAR motif.

To assess whether the retrieved preys that did not pass our stringent cut-offs, nonetheless represent true potential interactors of NINJA and N-TPL, additional Y2H experiments were carried out. For NINJA, the first four potential interaction partners with $SNR_{NINJA/EMPTY}$>7.2 and $FPKM_{NINJA}$<100 were tested in a binary Y2H assay (Table 3 and Figure 8). However, none of them showed interaction with NINJA, indicating that the installed threshold of $SNR_{NINJA/EMPTY}$>7.2 and $FPKM_{NINJA}$ >100 served as a good selection criterion, at least for NINJA.

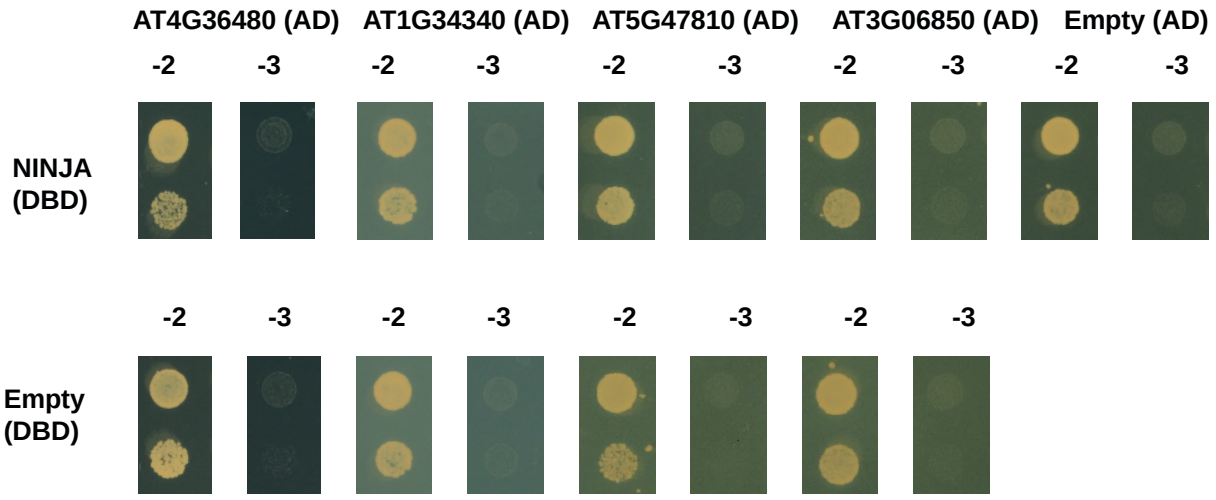

411

412 **Figure 8. Y2H analysis of potential interaction partners of NINJA.** Y2H analysis of NINJA, fused to the
413 DBD, and potential interaction partners, fused to the AD of the GAL4 TF, grown on selective medium
414 SD-Leu-Trp-His (-3). Transformed PJ69-4α yeast strains were also grown on SD-Leu-Trp (-2) medium
415 confirm growth capacity. No direct interactions could be observed for retrieved preys below the
416 threshold of $SNR_{NINJA/EMPTY}$>7.2 and $FPKM_{NINJA}$ values>100. Interaction between TPL and AT2G33550
417 had previously also been detected in the TOPLESS Interactome Y2H screen [18].
418

419 In the retained list of potential interactors using threshold $SNR_{TPL\text{-}N/EMPTY}$>6 with $FPKM_{N\text{-}TPL}$>100
420 values, the one candidate ATCKA2 (AT3G50000) that did not contain an EAR-domain was
421 tested for direct interaction with N-TPL in a Y2H assay, besides five candidates with $FPKM_{N\text{-}TPL}$<100
422 (Table 4 and Figure 9). For the latter set, we specifically avoided to pick candidates
423 from the AGL and IAA families, which are most likely true, but less abundant interactors, and
424 chose both candidates with and without an EAR domain. ATCKA2 interaction with N-TPL
425 could not be confirmed with binary Y2H, suggesting it was a false positive caused by the Y2H-
426 seq pipeline. In contrast however, interaction between TPL-N and the five other candidates
427 were all confirmed, demonstrating that they do not represent artefacts of the Y2H-seq
428 methodology and may be true interactors. Hence, in contrast to NINJA, this implicates that
429 the arbitrary threshold of $SNR_{TPL\text{-}N/EMPTY}$>6 with $FPKM_{N\text{-}TPL}$>100 was too stringent for N-TPL.
430 Perhaps this may be due to the pleiotropic function of TPL, which has an exceptionally high
431 number of protein interactors, often from multigene families. For proteins such as NINJA,

with a more defined role and a well-defined set of interactors, a stricter threshold may be justified. For proteins such as TPL, one may need to be more relaxed in determining candidate interactors. As exemplified here, this leads to the identification of potential novel interactors from gene families previously unreported to be capable of interacting with TPL, including EAR-domain containing proteins such as the RING/U-box protein AT3G05670, or proteins that do not contain an EAR domain such as the putative TF AT3G54390, the homeodomain TF AT2G40260 and the bHLH TF AT3G19860 (Table 4 and Figure 9).

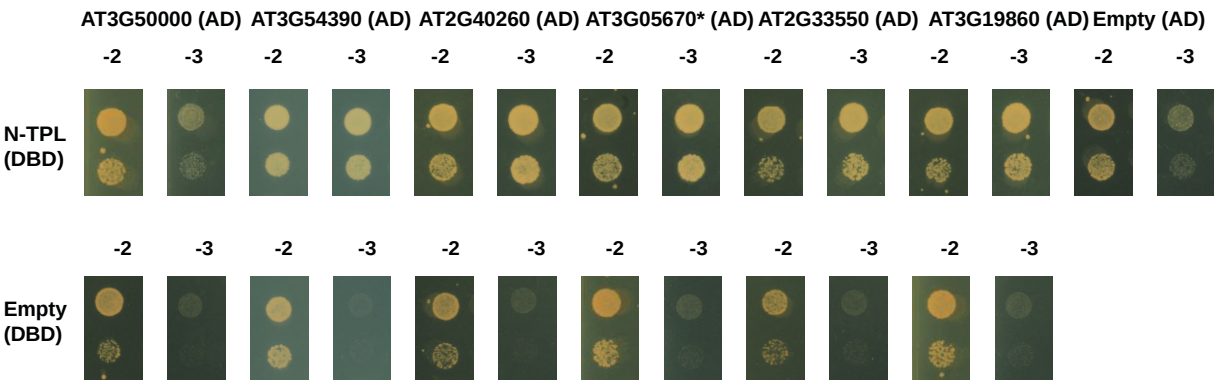

Figure 9. Binary Y2H validation of potential interaction partners of N-TPL. Y2H analysis of N-TPL, fused to the DBD, and potential interaction partners, fused to the AD of the GAL4 TF, grown on selective medium SD-Leu-Trp-His (-3). Co-transformed PJ69-4α yeast strains were also grown on SD-Leu-Trp (-2) medium to confirm growth capacity. No direct interaction was confirmed between ATCKA2 encoded by AT3G5000 and N-TPL, in contrast to the interactions with all other potential interactors selected from the list with a threshold of $SNR_{NINJA/EMPTY}$>7.2 and $FPKM_{NINJA}$<100 values. * indicates a truncated version of the protein, as it was present in the Y2H cDNA library.

Discussion

Here, we present a newly designed high-throughput Y2H-seq strategy to identify PPIs, which enables exploiting the full qualitative and quantitative potential of Y2H library screenings in an unprecedented way. Our method circumvents multiple shortcomings of a conventional Y2H library screening. As such, for instance consumable and DNA sequencing costs are significantly cut by using a pool-based NGS-strategy instead of the conventional isolation,

455 manipulation and sequencing of individual yeast clones that survive the screening selection.
456 Moreover, a higher sensitivity can be achieved in our Y2H-seq strategy through maximal
457 coverage of PPIs by increasing library titers. Consequently, interactions with less abundant
458 proteins that would be masked or lost in conventional Y2H screenings can now be detected.
459 In this regard, a factor that will determine the impact of future Y2H-seq screenings more
460 than ever, will be the choice and the quality of the Y2H cDNA library. For instance, full-length
461 protein libraries may mask PPIs by steric hindrance, hence the use of more complex Y2H
462 cDNA libraries encoding protein fragments as well as full-length proteins may now be
463 considered, and screened in one effort, which could lead to a comprehensive coverage of
464 the PPI space. The utility of fragment-based Y2H approaches has previously been
465 demonstrated [44,45]. By playing with sample preparations to generate cDNA libraries, one
466 could increase the genome coverage with no extra effort in the Y2H screening. For instance,
467 different organs from a single plant, different developmental stages of a single organ, or
468 explants subjected to different environmental cues or chemicals can now be pooled in a
469 single cDNA library. This will allow expanding the number of genes screened in a single
470 event, as well as different versions of the same gene, e.g. following expression after
471 alternative splicing or translation start events. As such, the Y2H-seq strategy will provide an
472 effective way to discover differentially regulated PPIs, allowing further exploration of
473 biological pathways and their regulation. Furthermore, the use of cDNA libraries makes it
474 possible to identify novel interaction partners of organisms of which the genome has not
475 been fully annotated yet, unlike the use of ORF libraries based on known and completely
476 fixed gene models.

477 The Y2H-seq strategy implements a quantitative readout system, with a straightforward
478 and adaptable scoring procedure. The use of background controls reliably allows eliminating

false positives in early stage. This does not only involve comparing quantitative NGS readouts from Y2H-seq screenings with bait proteins to those of control screenings with 'empty' control vectors, but also comparing the readouts of the screenings with bait proteins among each other. Indeed, as is also the case with other PPI discovery methods, such as tandem affinity purification [46,47], a specific 'blacklist' of returning Y2H-seq interactors for each cDNA library can be composed by marking common interactors of seemingly unrelated bait proteins. This may allow fine-tuning the thresholds to be set up in the filtering of the Y2H-seq NGS data, and thereby enable determining robust priority lists and reducing laborious and needless downstream validation assays to a minimum.

Finally, this strategy can also easily be extended to Y1H screenings, for which the same cDNA library could be screened, but for which considerably higher false-positive rates are typically obtained as compared to Y2H screenings [48,49]. As such, we anticipate that the cost and labor reduction along with the increased detection and quantification potential of our Y2H-seq strategy can give an important upgrade to this long-existing, but far from fully exploited screening tool.

Supporting information

S1 Table. Yeast strains generated in this study.

(DOCX)

S2 Table. Primers used in this study.

(DOCX)

501 ## Acknowledgements

502 We thank Annick Bleys for helping to prepare the manuscript and Frederik Coppens for
503 helpful advice on NGS. This research was supported by the Research Foundation Flanders for
504 postdoctoral fellowships to J.P. and L.P., the Program Ciências Sem Fronteiras for a
505 predoctoral fellowship to B.R. (Grant 201135/2014-0), the BEC.AR program for overseas
506 training of Argentine professionals in the fields of science, technology and productive
507 innovation for a scholarship to M.P. and the Special Research Fund from Ghent University
508 (project O1J14813).

509

510

511 ## References

512 1. Stynen B, Tournu H, Tavernier J, Van Dijck P (2012) Diversity in genetic *in vivo* methods for
513 protein-protein interaction studies: from the yeast two-hybrid system to the
514 mammalian split-luciferase system. Microbiol Mol Biol Rev 76: 331-382.

515 2. Xing S, Wallmeroth N, Berendzen KW, Grefen C (2016) Techniques for the analysis of
516 protein-protein interactions in vivo. Plant Physiol 171: 727-758.

517 3. Dunham WH, Mullin M, Gingras AC (2012) Affinity-purification coupled to mass
518 spectrometry: basic principles and strategies. Proteomics 12: 1576-1590.

519 4. Bensimon A, Heck AJR, Aebersold R (2012) Mass spectrometry–based proteomics and
520 network biology. Annu Rev Biochem 81: 379-405.

521 5. Dedecker M, Van Leene J, De Jaeger G (2015) Unravelling plant molecular machineries
522 through affinity purification coupled to mass spectrometry. Curr Opin Plant Biol 24: 1-
523 9.

524 6. Remy I, Michnick SW (2015) Mapping biochemical networks with protein fragment
525 complementation assays. Methods Mol Biol 1278: 467-481.

526 7. Kaushansky A, Allen JE, Gordus A, Stiffler MA, Karp ES, et al. (2010) Quantifying protein–
527 protein interactions in high throughput using protein domain microarrays. Nat Protoc
528 5: 773-790.

529 8. Johnsson N, Varshavsky A (1994) Split ubiquitin as a sensor of protein interactions in vivo.
530 Proc Natl Acad Sci USA 91: 10340-10344.

531 9. Kittanakom S, Chuk M, Wong V, Snyder J, Edmonds D, et al. (2009) Analysis of membrane
532 protein complexes using the split-ubiquitin membrane yeast two-hybrid system.
533 Methods Mol Biol 548: 247-271.

534 10. Müller J, Johnsson N (2008) Split-ubiquitin and the split-protein sensors: chessman for the
535 endgame. ChemBioChem 9: 2029-2038.

536 11. Fields S, Song O-k (1989) A novel genetic system to detect protein–protein interactions.
537 Nature 340: 245-246.

538 12. Häuser R, Stellberger T, Rajagopala SV, Uetz P (2012) Matrix-based yeast two-hybrid screen
539 strategies and comparison of systems. Methods Mol Biol 812: 1-20.

540 13. Yu H, Tardivo L, Tam S, Weiner E, Gebreab F, et al. (2011) Next-generation sequencing to
541 generate interactome datasets. Nat Methods 8: 478-480.

542 14. Weimann M, Grossmann A, Woodsmith J, Özkan Z, Birth P, et al. (2013) A Y2H-seq
543 approach defines the human protein methyltransferase interactome. Nat Methods 10:
544 339-342.

15. Yachie N, Petsalaki E, Mellor JC, Weile J, Jacob Y, et al. (2016) Pooled-matrix protein interaction screens using Barcode Fusion Genetics. Mol Syst Biol 12: 863.

16. Trigg SA, Garza RM, MacWilliams A, Nery JR, Bartlett A, et al. (2017) CrY2H-seq: a massively multiplexed assay for deep-coverage interactome mapping. Nat Methods 14: 819-825.

17. Pauwels L, Barbero GF, Geerinck J, Tilleman S, Grunewald W, et al. (2010) NINJA connects the co-repressor TOPLESS to jasmonate signalling. Nature 464: 788-791.

18. Causier B, Ashworth M, Guo W, Davies B (2012) The TOPLESS interactome: a framework for gene repression in Arabidopsis. Plant Physiol 158: 423-438.

19. Lynch TJ, Erickson BJ, Miller DR, Finkelstein RR (2017) ABI5-binding proteins (AFPs) alter transcription of ABA-induced genes via a variety of interactions with chromatin modifiers. Plant Mol Biol 93: 403-418.

20. Uhrig JF, Huang L-J, Barghahn S, Willmer M, Thurow C, et al. (2017) CC-type glutaredoxins recruit the transcriptional co-repressor TOPLESS to TGA-dependent target promoters in *Arabidopsis thaliana*. Biochim Biophys Acta - Gene Regul Mech 1860: 218-226.

21. Goralogia GS, Liu Tk, Zhao L, Panipinto PM, Groover ED, et al. (2017) CYCLING DOF FACTOR 1 represses transcription through the TOPLESS co-repressor to control photoperiodic flowering in Arabidopsis. Plant J 92: 244-262.

22. Espinosa-Ruiz A, Martínez C, de Lucas M, Fàbregas N, Bosch N, et al. (2017) TOPLESS mediates brassinosteroid control of shoot boundaries and root meristem development in *Arabidopsis thaliana*. Development 144: 1619-1628.

23. Graeff M, Straub D, Eguen T, Dolde U, Rodrigues V, et al. (2016) MicroProtein-mediated recruitment of CONSTANS into a TOPLESS trimeric complex represses flowering in Arabidopsis. PLoS Genet 12: e1005959.

24. Oh E, Zhu J-Y, Ryu H, Hwang I, Wang Z-Y (2014) TOPLESS mediates brassinosteroid-induced transcriptional repression through interaction with BZR1. Nat Commun 5: 4140.

25. Szemenyei H, Hannon M, Long JA (2008) TOPLESS mediates auxin-dependent transcriptional repression during *Arabidopsis* embryogenesis. Science 319: 1384-1386.

26. Nagels Durand A, Moses T, De Clercq R, Goossens A, Pauwels L (2012) A MultiSite Gateway™ vector set for the functional analysis of genes in the model *Saccharomyces cerevisiae*. BMC Mol Biol 13: 30.

27. Cuéllar Pérez A, Pauwels L, De Clercq R, Goossens A (2013) Yeast two-hybrid analysis of jasmonate signaling proteins. Methods Mol Biol 1011: 173-185.

28. James P, Halladay J, Craig EA (1996) Genomic libraries and a host strain designed for highly efficient two-hybrid selection in yeast. Genetics 144: 1425-1436.

579 29. Hellemans J, Mortier G, De Paepe A, Speleman F, Vandesompele J (2007) qBase relative
580 quantification framework and software for management and automated analysis of
581 real-time quantitative PCR data. Genome Biol 8: R19.

582 30. Bolger AM, Lohse M, Usadel B (2014) Trimmomatic: a flexible trimmer for Illumina
583 sequence data. Bioinformatics 30: 2114-2120.

584 31. Gnimpieba EZ (2013) RNA-Seq workflow with TopHat and Cufflinks using Bioextract Server.
585 Available at: http://wwwmyexperimentorg/workflows/3895html?version=1.

586 32. Chini A, Gimenez-Ibanez S, Goossens A, Solano R (2016) Redundancy and specificity in
587 jasmonate signalling. Curr Opin Plant Biol 33: 147-156.

588 33. Goossens J, Fernández-Calvo P, Schweizer F, Goossens A (2016) Jasmonates: signal
589 transduction components and their roles in environmental stress responses. Plant Mol
590 Biol 91: 673-689.

591 34. Cuéllar Pérez A, Nagels Durand A, Vanden Bossche R, De Clercq R, Persiau G, et al. (2014)
592 The non-JAZ TIFY protein TIFY8 from *Arabidopsis thaliana i*s a transcriptional repressor.
593 PLoS ONE 9: e84891.

594 35. Chico JM, Chini A, Fonseca S, Solano R (2008) JAZ repressors set the rhythm in jasmonate
595 signaling. Curr Opin Plant Biol 11: 486-494.

596 36. Vanholme B, Grunewald W, Bateman A, Kohchi T, Gheysen G (2007) The tify family
597 previously known as ZIM. Trends Plant Sci 12: 239-244.

598 37. Gonzalez N, Pauwels L, Baekelandt A, De Milde L, Van Leene J, et al. (2015) A repressor
599 protein complex regulates leaf growth in Arabidopsis. Plant Cell 27: 2273-2287.

600 38. Kazan K, Manners JM (2013) MYC2: the master in action. Mol Plant 6: 686-703.

601 39. Goossens J, Swinnen G, Vanden Bossche R, Pauwels L, Goossens A (2015) Change of a
602 conserved amino acid in the MYC2 and MYC3 transcription factors leads to release of
603 JAZ repression and increased activity. New Phytol 206: 1229-1237.

604 40. Gasperini D, Chételat A, Acosta IF, Goossens J, Pauwels L, et al. (2015) Multilayered
605 organization of jasmonate signalling in the regulation of root growth. PLoS Genet 11:
606 e1005300.

607 41. Acosta IF, Gasperini D, Chételat A, Stolz S, Santuari L, et al. (2013) Role of NINJA in root
608 jasmonate signaling. Proc Natl Acad Sci USA 110: 15473-15478.

609 42. Gietz RD (2014) Yeast transformation by the LiAc/SS carrier DNA/PEG method. Methods
610 Mol Biol 1163: 33-44.

611 43. Kazan K (2006) Negative regulation of defence and stress genes by EAR-motif-containing
612 repressors. Trends Plant Sci 11: 109-112.

613 44. Boxem M, Maliga Z, Klitgord N, Li N, Lemmens I, et al. (2008) A protein domain-based
614 interactome network for *C. elegans* early embryogenesis. Cell 134: 534-545.

615 45. Waaijers S, Koorman T, Kerver J, Boxem M (2013) Identification of human protein
616 interaction domains using an ORFeome-based yeast two-hybrid fragment library. J
617 Proteome Res 12: 3181-3192.

618 46. Van Leene J, Eeckhout D, Cannoot B, De Winne N, Persiau G, et al. (2015) An improved
619 toolbox to unravel the plant cellular machinery by tandem affinity purification of
620 *Arabidopsis* protein complexes. Nat Protoc 10: 169-187.

621 47. Goossens J, De Geyter N, Walton A, Eeckhout D, Mertens J, et al. (2016) Isolation of protein
622 complexes from the model legume *Medicago truncatula* by tandem affinity
623 purification in hairy root cultures. Plant J 88: 476-489.

624 48. Li JJ, Herskowitz I (1993) Isolation of ORC6, a component of the yeast origin recognition
625 complex by a one-hybrid system. Science 262: 1870-1874.

626 49. Wang MM, Reed RR (1993) Molecular cloning of the olfactory neuronal transcription factor
627 Olf-1 by genetic selection in yeast. Nature 364: 121-126.

628 # Supporting information

629 **S1 Table. Yeast strains generated in this study.**

Strains generated for binary Y2H assays
PJ69-4α; pDEST32[**TPL-N**];pDEST22[IAA17]
PJ69-4α; pDEST32[**TPL-N**];pDEST22[NINJA]
PJ69-4α; pDEST32[**TPL-N**];pDEST22[EMPTY]
PJ69-4α; pDEST32[NINJA];pDEST22[PPD1]
PJ69-4α; pDEST32[NINJA];pDEST22[JAZ1]
PJ69-4α; pDEST32[NINJA];pDEST22[JAZ2]
PJ69-4α; pDEST32[NINJA];pDEST22[JAZ4]
PJ69-4α; pDEST32[NINJA];pDEST22[EMPTY]
Strains generated for Y2H-seq screening
PJ69-4α; pDEST32[TPL-N]
PJ69-4α; pDEST32[NINJA]
PJ69-4α; pDEST32[EMPTY]

630

631 **S2 Table. Primers used in this study.**

Description	Sequence
IAA17 (AT1G04250) cloning primer Fw	5’- AAAAAGCAGGCTCCATGATGGGCAGTGTCGAGCT-3’
IAA17 (AT1G04250) cloning primer Rv	5´-AGAAAGCTGGGTCTCMAGCTCTGCTCTTGCACTTCT-3’
JAZ1 (AT1G19180) qPCR primer Fw	5’- TTCTGAGTTCGTCGGTAGCC -3’
JAZ1 (AT1G19180) qPCR primer Rv	5’- CACGTCTGTGAGAAGCTAGGC -3’
JAZ2 (AT1G74950) qPCR primer Fw	5’- CTCTTTAGCCTGCGAACTCC -3’

JAZ2 (AT1G74950) qPCR primer Rv	5’- TTGGTATGGTGCCTTTGATG -3’
JAZ5 (AT1G17380) qPCR primer Fw	5’- AAAGATGTTGCTGACCTCAGTG -3’
JAZ5 (AT1G17380) qPCR primer Rv	5’- CCCTCCGAAGAATATGGTCA -3’
JAZ6 (AT1G72450) qPCR primer Fw	5’- TTCATCGATTCTTTGCTAAACG -3’
JAZ6 (AT1G72450) qPCR primer Rv	5’- ATCGATGGAGCAACCATCTC -3’
JAZ7 (AT2G34600) qPCR primer Fw	5’-ATGCGACTTGGAACTTCGCCTT-3’
JAZ7 (AT2G34600) qPCR primer Rv	5’-AGAGCTGCTTGATTCGTCCAACG-3’
JAZ8 (AT1G30135) qPCR primer Fw	5’-CGATCGCAAGCAGAGAAATG-3’
JAZ8 (AT1G30135) qPCR primer Rv	5’-GATCCGACCCGTTTGAGGAT-3’
JAZ12 (AT5G20900) qPCR primer Fw	5’- CATCTAATGTGGCATCACCAG -3’
JAZ12 (AT5G20900) qPCR primer Rv	5’- TGCCTCCTTGCAATAGGTAGA -3’
NINJA (AT4G28910) qPCR primer Fw	5’-AAGTGATTCGGGTCAACAGC-3’
NINJA (AT4G28910) qPCR primer Rv	5’-GGTTGGAAGAAGAACCACCA-3’
PEAPOD1 (AT4G14713) qPCR primer Fw	5’-AAAGATGGCCACAAGACGAC-3’
PEAPOD1 (AT4G14713) qPCR primer Rv	5’-GGACACTTTTTGGCCTTTGA-3’
AZF2 (AT3G19580) qPCR primer Fw	5’-ATTCAACAGCTCCGACCATC-3’
AZF2 (AT3G19580) qPCR primer Rv	5’-GGCTCCTTTCTTCCGATACC-3’
KIX9 (AT4G32295) qPCR primer Fw	5’-ATCATGTATTCCAAAGCCAATTC-3’
KIX9 (AT4G32295) qPCR primer Rv	5’-CGGTCTAAAAGGGTCTTCATGT-3’
TIFY8 (AT4G32570) qPCR primer Fw	5’-CGTCTCCGACAGACAGAACA-3’
TIFY8 (AT4G32570) qPCR primer Rv	5’-CCTGAAAACCGATTGCTCAT-3’
IAA30 (AT3G62100) qPCR primer Fw	5’-TTCAATGCTTCAATCCTTTGG-3’
IAA30 (AT3G62100) qPCR primer Rv	5’-AGCACGTGACTCTTCTCACTACA-3’
GAL4AD pDEST22 Rv	5’-GGTTTGGTGGGGTATCTTCA-3’
pDEST22 Fw Sanger sequencing	5’-TATAACGCGTTTGGAATCACT-3’

pDEST22 Rv Sanger sequencing	5’-AGCCGACAACCTTGATTGGAGAC-3’

632

633

634

635